Tech Science Press

Biocomposites Based on Thermoplastic Starch and Granite Sand Quarry Waste

María G. Passaretti[1,2,*], Mario D. Ninago[3,4], Cecilia I. Paulo[5], Horacio A. Petit[5], Edgardo F. Irassarc[5], Daniel A. Vega[6], Marcelo A. Villar[1,2] and Olivia V. López[1]

[1]Planta Piloto de Ingeniería Química, PLAPIQUI (UNS-CONICET), Camino ''La Carrindanga'' Km 7, Bahía Blanca, 8000, Buenos Aires, Argentina.

[2]Departamento de Ingeniería Química, Universidad Nacional del Sur (UNS), Bahía Blanca, 8000, Buenos Aires, Argentina.

[3]Facultad de Ciencias Aplicadas a la Industria (FCAI), Universidad Nacional de Cuyo (UNCuyo), Bernardo de Irigoyen 375, San Rafael, 5600, Mendoza, Argentina.

[4]Consejo Nacional de Investigaciones Científicas y Técnicas (CONICET), Godoy Cruz 2290, Ciudad Autónoma de Buenos Aires, C1425FQB, Buenos Aires, Argentina.

[5]Facultad de Ingeniería, Universidad Nacional del Centro de la Provincia de Buenos Aires (UNCPBA). Centro de Investigaciones en Física e Ingeniería, CIFICEN (UNCPBA-CICPBA-CONICET), 7400, Olavarría, Argentina.

[6]Instituto de Física del Sur, IFISUR (UNS-CONICET), Bahía Blanca, 8000, Argentina.

[*]Corresponding Author: María G. Passaretti. Email: mgpassaretti@plapiqui.edu.ar.

Abstract: Granite stone is a by-product of the rock crushing manufacturing. An industrial waste in powder form that causes health problems and environmental pollution. Fine particles fraction can be used as a partial replacement of sand in concrete manufacture. In this work, an alternative exploitation of this waste fraction is proposed. Granite sand (GS) with particles mean size of ~1 μm was employed as thermoplastic starch (TPS) filler at different concentrations. Biocomposites were obtained by melt-mixing and thermo-compression, achieving translucent and easy to handle films. A good GS dispersion within the matrix was evidenced by SEM. Mineral presence induced a shift of starch's melting point to higher values and a better thermal resistance. TPS UV absorption capacity was increased ~90% by GS addition. An increment in TPS Young's modulus and maximum tensile stress of 5 and 3 times, respectively was observed by adding 5 % w/w GS.

Keywords: Thermoplastic starch; granite sand; melt processing; final properties

1 Introduction

Over the last decade, the interest in composite materials based on natural polymers has increased due to their renewable origin, biodegradability, and wide variety of industrial applications. Within this context, starch is an attractive alternative because it is relatively inexpensive, biodegradable, nontoxic, and it can be converted into a thermoplastic material. Several authors reported studies about thermoplastic starch plasticized by different additives [1-5]. Incorporation of inorganic particles into organic polymer matrices allows obtaining organic-inorganic composites. Mineral fillers have often shown to improve physical, mechanical, and thermal properties of TPS composites. Despite that numerous studies reporting the use of several inorganic fillers of starch materials can be found in the literature, publications employing mineral wastes are scarce. The use of industrial residues as fillers of biocomposites has an economical benefit, with the resultant attenuation of waste volumes.

Argentina has large companies dedicated to the extraction of industrial minerals, reaching about 755 mining ventures. In order of importance, produces sand for construction (mainly crushing sands), crushed stone, boulder, limestone, coarse, and travertine, among others. Crushing sand production in 2015 reached a volume of 43 million tons, with an increment of 4% respect to 2014, driven by the construction sector [6].

DOI: 10.32604/jrm.2019.04281

Granite sand (GS) is an industrial waste, which is obtained from the granite polishing industry. Due to its powder form, it would be easily carried away by air and it will cause health problems and environmental pollution. Therefore, it is highly desirable to find uses in an effective manner to minimize these damages. Besides, this will reduce pressure on finding new dumping grounds for these wastes [7]. One of the most studied applications of GS is as fine aggregate in concrete industry, partially replacing natural river sand. Important features for this use is its inertness and angular surfaces, which provides more specific area imparting better bonding characteristics [8]. Other less explored use for GS would be as filler agent of polymeric matrices.

Granite sand is a mixture of different minerals, composed by muscovite, orthoclase, quartz, and biotite, among others. Particularly, muscovite is a laminar silicate of the micas-clays family [9,10]. Its structure permits the intercalation of organic-inorganic species between mineral slabs, which makes muscovite an excellent filler for polymeric materials [11]. Several authors have reported the potential use of muscovite as reinforcement of thermoplastic materials [12-14].

The aim of this work was to obtained biocomposites materials based on thermoplastic corn starch (TPS) and granite sand (GS). The effect of concentration of GS on final properties of TPS films was studied by complementary techniques.

2 Materials and Methods

2.1 Materials

Native corn starch was provided by Misky-Arcor (Tucumán, Argentina) with an amylose content of 23.9 ± 0.7%, previously characterized by López et al. [15]. This polysaccharide presents an average molar mass of $2 \cdot 10^4$ g·mol^{-1} for amylose and $2 \cdot 10^5$-$1 \cdot 10^6$ g·mol^{-1} for amylopectin [16]. Analytical grade glycerol (Anedra, Argentina) was used as starch plasticizer.

Granite sand (GS) was provided by a quarry located in Olavarría (Buenos Aires-Argentina), with a mean size of ~ 6 mm. This sample was sun-dried and grounded in a pilot scale ball mill (TecMaq MBL300, balls size: 1.5 cm and 2.5 cm) during 150 minutes.

2.2 Granite Sand Characterization

Fourier Transform Infrared (FTIR) spectrum was obtained using a Thermo Nicolet Nexus spectrophotometer (United States). Sample was prepared by mixing GS as fine powder with KBr (99% Sigma Aldrich, United States) at 1 % w/w. The mixture was pressed and a transparent disk was obtained. FTIR spectrum was recorded at 4 cm^{-1} resolution over the 4000-400 cm^{-1} range, using an accumulation of 64 scans and air as background.

Particles microstructure was characterized by Scanning Electron Microscopy (SEM), using a JEOL JSM-35 CF electron microscope (Japan) with a secondary electron detector. GS particles were dispersed over 3M® aluminum conductive tape by using an air flow and mounted onto bronze stubs. Then, they were coated with a gold layer, employing an argon plasma metallizer (sputter coater PELCO 91000).

2.3 Thermoplastic Starch-Granitic Sand Composites

Films preparation

Mixtures of native corn starch, glycerol (30%, w/w), and granitic sand (0, 1, and 5 % w/w) were prepared. Granitic sand was premixed with starch to achieve good particles dispersion between both powders. Then, glycerol was added and samples were processed in an Atlas Laboratory mini mixer at 140ºC and 50 rpm for 15 min. Films were obtained by thermo-compression using a hydraulic press at 150 kg cm^{-2} and 140ºC for 6 min. Composites films were named as TPS_{0GS}, TPS_{1GS}, and TPS_{5GS}.

Films characterization

Films homogeneity and appearance were examined by Scanning Electronic Microscopy (SEM). Studies were performed in a JEOL JSM-35 CF electron microscope (Japan), with a secondary electron

detector. Films were cryo-fractured by immersion in liquid nitrogen, mounted on bronze stubs and coated with a gold layer, using an argon plasma metallizer (sputter coater PELCO 91000-California, United States). Thus, film surfaces and their cross-sections were satisfactorily observed.

Degradation tests were carried out in a thermogravimetric balance TA Instrument Discovery Series (New Castle, United States). Samples were heated from 30ºC to 700ºC at 10 ºC min^{-1}, under nitrogen flow. Curves of mass as a function of temperature were recorded and the decomposition temperature at 50% mass loss (DT50%) was acquired from the first derivative curves (DTG).

Differential scanning calorimetry (DSC) was performed on a Discovery DSC (TA Instruments, USA) under nitrogen atmosphere. Approximately, 10 mg of each sample was tested and heated from 50ºC to 250ºC at 10 ºC min^{-1}. An empty hermetic pan was used as reference. From the thermograms, the following parameters were obtained: onset (T_o) and melting (T_m) temperatures, and melting enthalpy (ΔH_m).

Opacity and UV barrier capacity were determined from the absorbance spectra (200-750 nm) recorded in a Shimadzu UV-160 spectrophotometer (Columbia, United States). Films were placed on the internal side of a quartz spectrophotometer cell. Film opacity (AU nm) was defined as the area under the recorded curve determined by an integration procedure according to Piermaría et al. [17], and the standard test method for haze and luminous transmittance of transparent plastics recommendations (ASTM D1003-00).

Films color measurements were performed using a Hunterlab UltraScan XE (Reston, US) colorimeter in the transmittance mode. Color parameters L*, a*, and b* were recorded according to the CieLab scale, in at least ten randomly selected positions for each film sample. Color parameters range from L* = 0 (black) to L* = 100 (white), -a* (greenness) to + a* (redness), and -b* (blueness) to + b* (yellowness). Besides Hue angle (H*) and Chroma (C*) were calculated using the following equations [18]:

$$H^* = \tan^{-1}\frac{b^*}{a^*} \quad (1)$$

$$C^* = \sqrt{a^{*2}+b^{*2}} \quad (2)$$

Mechanical behavior was measured in an Instron 3369 universal machine (Instron, USA) through tensile tests. For stress-strain tests, ten probes of 13 × 100 mm of each film formulation were assayed. Maximum tensile strength, elongation at break, and Young's modulus were calculated according to the ASTM D882-00.

Analysis of variance (ANOVA) was used to compare mean differences between properties of TPS matrix and TPS_{GS} composites. A comparison of mean values from UV/Vis, opacity and mechanical properties of the essayed samples was performed by Fisher's least significant difference test, conducted at a significance level p = 0.05.

3 Results and Discussion

3.1 Structural Characterization of Granite Sand (GS)

Figure 1a shows the FTIR spectra of granite sand, showing typical absorption bands of natural muscovite. In this sense, at 3430 cm^{-1} and 1640 cm^{-1} appear the signals associated to OH stretching vibration and OH deformation vibration of water. At 1015 cm^{-1} and 1067 cm^{-1} were detected a wide and a shoulder absorption bands attributed to Si-O stretching respectively. At 752 cm^{-1} it was detected a signal associated to Al-O-Al stretching in tetrahedral sheets. The signal located at 537 cm^{-1} is related to Al-O-Si with Al in octahedral sheets. Finally, the band at 472 cm^{-1} belonged to Si-O-Si deformation. Similar spectra for natural muscovite were reported by Friedrich et al. [19] and Jia et al. [10]. Fig. 1(b) shows SEM micrograph of GS evidencing particles morphology and dimensions. Morphology mainly depends on the source of the native stone and in this case, GS particles are irregular, angular, porous, and rough. Similar finding was reported by other authors [20-23].

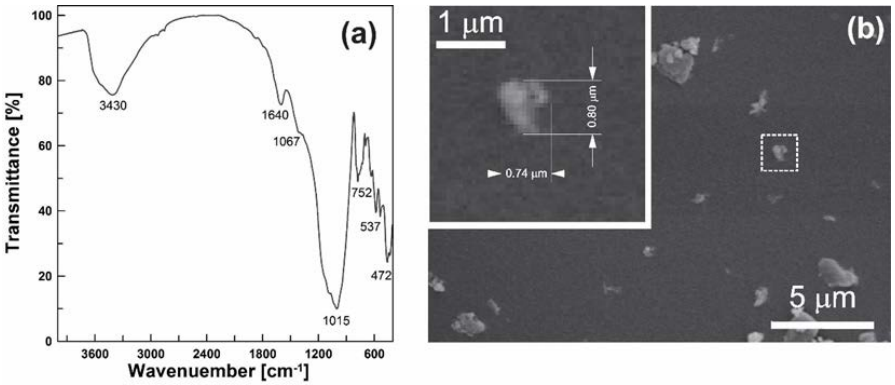

Figure 1: (a) FTIR spectra and (b) SEM micrograph of granite sand

3.2 Thermoplastic Starch-Granite Sand Composites

Starch melt-mixing, in the presence of glycerol and GS, allowed obtaining homogenous composite materials with thermoplastic properties. From processed composites, translucent films were obtained by thermo-compression.

Fig. 2 shows SEM micrographs of fracture surfaces of TPS films and their composites containing GS. Neat thermoplastic starch films (TPS_{0GS}) showed a continuous and smooth cross section without un-melted starch granules, indicating a good matrix integrity. Huang and Yu [4] pointed out that plasticizers penetrate inside corn starch granules during processing under temperature and shear stress, leading their disruption and forming a uniform continuous phase. Other authors reported a similar microstructure for thermoplastic starch films [24-26]. Regarding composite films, a good dispersion of GS within the matrix was evidence for both studied concentrations. Filler distribution can be appreciated in Fig. 2 for TPS_{5GS} composite. Fillers act efficiently as polymer reinforcement if they are well dispersed and the interface with the matrix is continuous [27]. The absence of pull-out phenomenon is an indication of a good interface adhesion between filler and matrix. Thus, it will be expected an increase in tensile strength of composites with the highest particles content. The partial hydrophilic character of this mineral filler (GS) favored its dispersion along the matrix. Müller, Laurindo and Yamashita [28] stressed that compatibility of starch matrix and nanoclays mainly depends on the filler hygroscopicity and concentration.

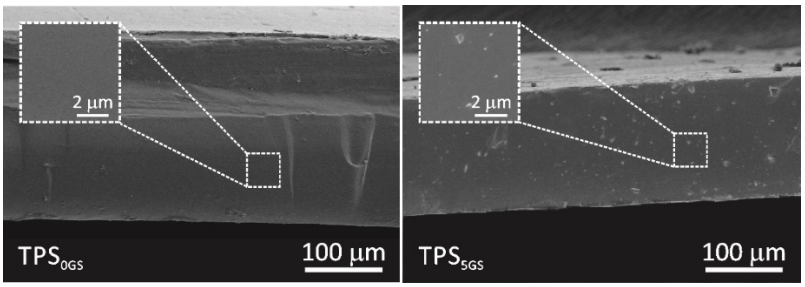

Figure 2: SEM micrographs of films based on thermoplastic starch (TPS_{0GS}) and TPS with 5 % w/w granite sand (TPS_{5GS})

TGA thermograms of TPS and its composites, as well as first derivative curves, are shown in Fig. 3. Despite the presence of GS, the behavior of mass loss curves was similar in all cases. The first mass loss step could be attributed to samples dehydration while, from 100ºC to the beginning of starch decomposition, the mass loss might be due to glycerol volatilization. In the second step, the mass loss occurred between 266ºC and 345ºC with peaks at 317ºC, 320ºC, and 321ºC for TPS_{0GS}, TPS_{1GS}, and TPS_{5GS}, respectively.

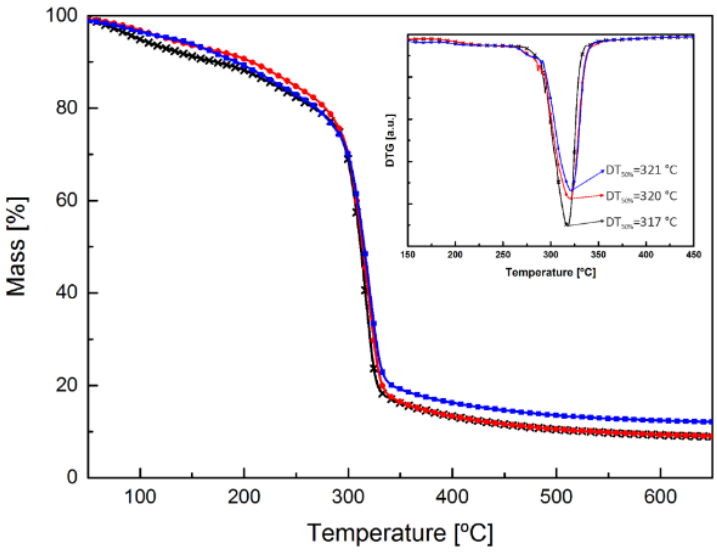

Figure 3: TG and DTG curves of films based on thermoplastic starch (TPS), and TPS with 1 and 5 % w/w of granite sand (GS). Symbols: TPS_{0GS}(x), TPS_{1GS} (●), TPS_{5GS} (■)

During this event, ether bonds and unsaturated structures are created by thermal condensation between hydroxyl groups of starch chains, removing water and other small molecules [29]. Comparing with organic materials, inorganic ones have better thermal stability and thermal resistant properties because of its configuration characteristics. Therefore, the introduction of inorganic particles will greatly improve the thermal stability of polymer materials [3]. Other authors reported a similar effect of mineral filler on thermal stability of starch based materials [3,28,30,31].

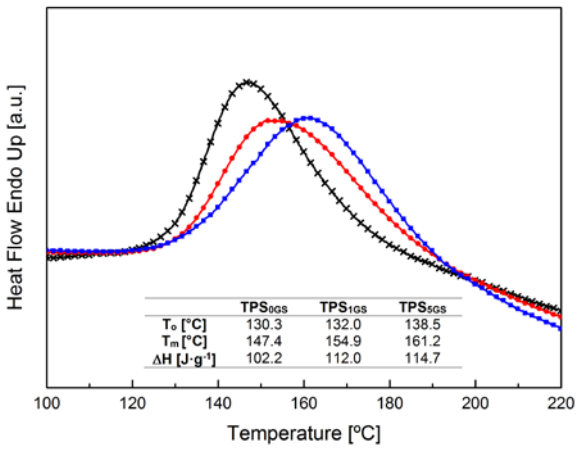

Figure 4: DSC curves of films based on thermoplastic starch (TPS), and TPS with 1 and 5 % w/w of granite sand (GS). Symbols: TPS_{0GS}(x), TPS_{1GS} (●), TPS_{5GS} (■)

DSC thermograms for all samples are depicted in Fig. 4. In this Figure is also included a table with thermal parameters such as onset and melting temperatures (T_o and T_m), as well as melting enthalpy (ΔH_m). DSC curves of TPS and its composite films showed a single transition that occurs over a quite broad temperature range (120-200ºC). Sun et al. [27] and Savadekar and Mhaske [32] reported similar results for composites based on thermoplastic starch films. This transition is an endothermic event which corresponds to the melting of starch's crystalline fraction. Fig. 4 shows a significant shift of starch's melting point towards higher values due to GS incorporation to TPS films. This effect could be attributed to the fact that

small and irregular GS particles were well distributed in the starch matrix. Therefore, the contact area between particles and matrix increased and lead to a more compact structure, which would require a higher melting temperature. Sun et al. [27] and Aila-Suárez et al. [33] presented a similar discussion for TPS composites containing $CaCO_3$ and cellulose nanoparticles, respectively. Regarding melting enthalpy, the incorporation of GS allowed increasing the value of this thermal parameter. For TPS_{1GS} and TPS_{5GS}, ΔH_m increased 10% and 13% respectively, compared to neat TPS. Sun et al. [27] attributed this increment to interactions between mineral particles and chain segments of TPS, which might increase films crystallinity. It could be assumed that the higher melting enthalpies, the higher TPS-GS compatibility.

Fig. 5 corresponds to UV-vis spectra of TPS films and its composites. In this figure, it is also represented UV barrier capacity and opacity in a bar plot. Opacity values were used to assess films transparency. Particularly, in the case of composites provide information about the filler size dispersed within the starch matrix. Thus, particle sizes larger than visible wavelengths would disperse light, leading to opaque materials [34].

As it was expected, neat TPS films have the lowest opacity values, increasing significantly with GS concentration in composite formulations. This effect of particles presence on the opacity of starch based composites was also reported by several authors [27,35,36]. Generally, opacity is a desirable property for films to be used as packaging since they are excellent barriers to prevent light-induced degradation of products. UV absorption of films was measured at a wavelength range from 252 nm to 300 nm (Fig. 5). The inherent UV absorption capacity of TPS films was improved by the addition of GS as filler. As it was discussed for opacity, the fact that films act as barrier against UV radiation, can be considered a beneficial property for several applications, including packaging for foods containing lipids, as well as for cosmetics and pharmaceutical products [37,38].

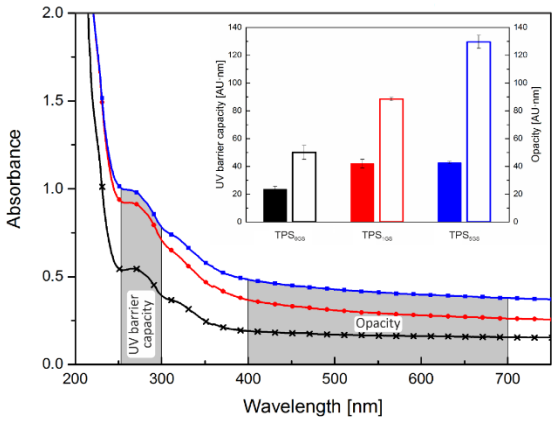

Figure 5: Absorption spectra, opacity (empty bars), and UV-barrier capacity (full bars) of thermoplastic starch (TPS), and TPS with 1 and 5% w/w of granite sand (GS). Symbols: TPS_{0GS} (x), TPS_{1GS} (●), TPS_{5GS} (■)

Plot included in Fig. 6 represents an orthogonal system of chromaticity parameters, a* (redness) and b* (yellowness). Values corresponding to TPS and its composites were all located in the first quadrant of this system. The low dispersion of the obtained results for every tested film is an indicative of the effective thermal processing for composite preparation, as well as the homogeneous filler distribution within TPS matrix, as it was observed by SEM. For each formulation, a circumference including a* and b* parameters were drawn in the orthogonal system. It was attempted to represent the color and luminosity of TPS_{0GS}, TPS_{1GS}, and TPS_{5GS}, by dyeing the circular zones considering not only the chromaticity parameters but also the luminosity values (L*). The presence of GS increased a* and b* values, respect to neat TPS. Regarding parameter a*, a slight increment was achieved; meanwhile for b* this change was more significant. Jafarzadeh et al. [39] reported similar findings for composites based on semolina flour with nano kaolin. Fig. 6 also included the values of L*, H*, and C* for all tested composites. Luminosity became progressively decreased

by higher GS content. This observation could be attributed to the inherent grey color of the mineral particles. Echeverría et al. [40] reported similar effect for montmorillonite incorporation to soy protein films. Hue angle (H*) describes the materials color tone and as it can be observe, no significant differences were detected among tested films. Regarding Chroma (C*), it indicates the separation between a specific color tone and a grey with the same luminosity and represents the hue saturation. Granitic sand addition increased C* parameter of TPS films, reaching the higher increment for TPS_{1GS}.

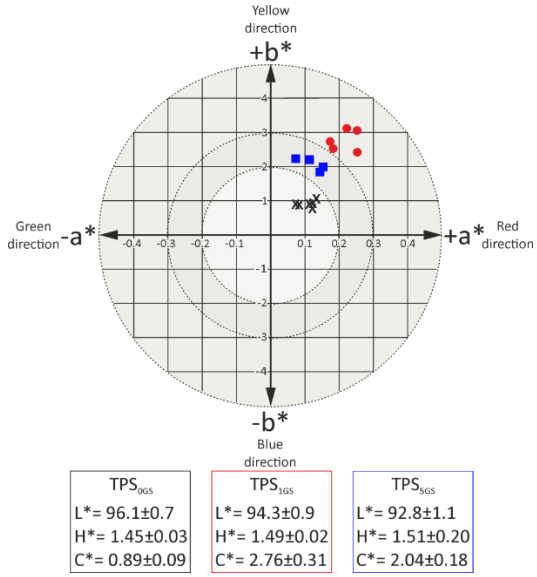

Figure 6: Orthogonal system of chromaticity parameters, a* (redness) and b* (yellowness), of thermoplastic starch (TPS), and TPS with 1 and 5 % w/w of granite sand (GS). Symbols: TPS_{0GS} (x), TPS_{1GS} (●), TPS_{5GS} (■)

Mechanical testing is considered relevant in evaluating elementary properties of new developing materials. Fig. 7 shows representatives stress-strain curves for neat TPS and its composite films. Maximum tensile strength, elongation at break, and Young´s modulus values of the tested films are included in the table inserted in Fig. 7. At the beginning, stress increases rapidly and it is proportional to the strain; this region corresponds to the elastic reversible strain area (elastic deformation). When the yield point is reached, plastic flow starts and the strain is no longer reversible (plastic strain area). During plastic flow period, the curve continuously bend away because of the increasing rate flow as stress is applied until the film's rupture [41]. Regarding the effect of GS addition on TPS mechanical properties, a progressive enhancement in maximum tensile strength and in Young's modulus was acquired along with a substantial decrease in elongation at break with the amount of filler in the matrix. The significant increment in the Young's modulus of 400% by adding 5 % w/w GS, could be attributed to the strong interfacial interactions among filler and matrix, as it was observed by SEM. According to de Melo et al. [25], the improvement on mechanical properties of starch composites by clay addition, might be due to the filler's rigidity and to the interactions between polymeric matrix and layered silicates via hydrogen bonds. In accordance with these results, Echeverría et al. [40] stressed that the complete dispersion of clay layers in a polymer must optimize the number of strengthening elements available to support a load and avoid cracks in the material, improving the mechanical properties.

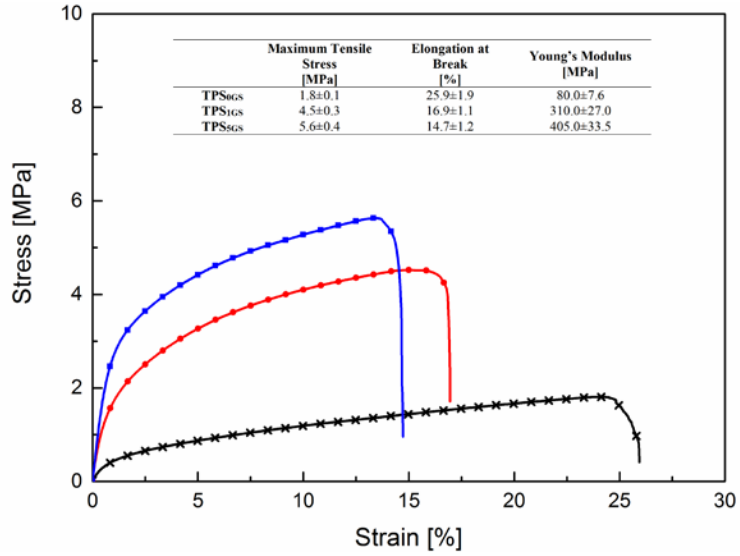

Figure 7: Stress-strain curves and mechanical properties of films based on thermoplastic starch (TPS), and TPS with 1 and 5 % w/w of granite sand (GS). Symbols: TPS_{0GS} (x), TPS_{1GS} (●), TPS_{5GS} (■)

4 Conclusions

Biocomposites materials were obtained from thermoplastic corn starch (TPS) and granite sand (GS) by melt-mixing and thermo-compression. Films resulted translucent, homogenous, and easy to handle. Thermal processing as well as the inherent particles and TPS characteristics, lead to an optimal filler distribution within the matrix. GS incorporation up to 5 % w/w, increased TPS thermal stability, meanwhile DSC parameters associated to TPS melting, shifted to higher values. Particles acted as blocking agents of UV-vis radiation, thus opacity and UV barrier capacity of TPS films were increased significantly. Regarding TPS mechanical properties, maximum tensile stress and Young's modulus increased 3 and 5 times respectively with the incorporation of 5 % w/w GS. However, particles presence reduced significantly TPS elongation at break. Exploitation of granite sand as TPS filler not only allows obtaining biocomposites with enhanced properties respect to the neat matrix, but also contributes to give added value to a quarry waste.

Acknowledgement: We express our gratitude to the Consejo Nacional de Investigaciones Científicas y Técnicas (CONICET, Argentina, Grant PIP 112-201501-00127), the Fondo para la Investigación Científica y Tecnológica (FONCYT, Grant PICT-2016-0181) and Universidad Nacional del Sur (UNS, Argentina, Grant PGI 24/M154) for their financial support.

References

1. Córdoba, A., Cuéllar, N., González, M., Medina, J. (2008). The plasticizing effect of alginate on the thermoplastic starch/glycerin blends. *Carbohydrate Polymers, 73(3),* 409-416.
2. Huang, M. F., Yu, J. G., Ma, X. F. (2004). Studies on the properties of Montmorillonite-reinforced thermoplastic starch composites *Polymer, 45(20),* 7017-7023.
3. Huang, M., Yu, J., Ma, X. (2006). High mechanical performance MMT-urea and formamide-plasticized thermoplastic cornstarch biodegradable nanocomposites. *Carbohydrate Polymers, 63(3),* 393-399.
4. Huang, M., Yu, J. (2006). Structure and properties of thermoplastic corn starch/montmorillonite biodegradable composites. *Journal of Applied Polymer Science, 99(1),* 170-176.
5. Zhang, Y., Rempel, C., Liu, Q. (2014). Thermoplastic starch processing and characteristics-a review. *Critical Reviews in Food Science and Nutrition, 54(10),* 1353-1370.
6. Méndez A, Martin, F. E., Gorzycki, R. (2016). Informes de Cadenas de Valor. https://www.economia.gob.ar/peconomica /docs/SSPE_Cadenas_de_valor_Renovables.pdf.

7. Ghannam, S. (2016). Comparison between concrete with granite powder and concrete with iron powder. *International Journal of Applied Engineering Research, 21,* 10501-10515.
8. Rao, B. K., Desai, B. V., Mohan, J. D. (2012). Probabilistic analysis of mode II fracture of concrete with crushed granite stone fine aggregate replacing sand. *Materials Research, 15(1),* 41-50.
9. Barlow, S. G., Manning, D. A. C., Al, S. (1999). Influence of time and temperature on reactions and transformations of muscovite mica. *British Ceramic Transactions, 98(3),* 122-126.
10. Jia, F., Su, J., Song, S. (2015). Can natural muscovite be expanded? *Colloids and Surfaces A: Physicochemical and Engineering Aspects, 471,* 19-25.
11. Santos, S. F., França, S. C. A., Ogasawara, T. (2011). Method for grinding and delaminating muscovite. *Mining Science and Technology, 21(1),* 7-10.
12. Ismail, N. H., Bakhtiar, N. S. A., Akil, H. (2017). Effects of cetyltrimethylammonium bromide (CTAB) on the structural characteristic of non-expandable muscovite. *Materials Chemistry and Physics, 196,* 324-332.
13. Sodergard, A., Ekman, K., Stenlund, B., Lassas, A. C. (1996). The influence of EB-crosslinking on barrier properties of HDPE-mica composites. *Applied Polymer Science, 59,* 1709-1714.
14. Zhao, R., Huang, J., Sun, B., Dai, G. (2001). Study of the mechanical properties of mica-filled polypropylene-based GMT composite. *Journal of Applied Polymer Science, 82(11),* 2719-2728.
15. López, O. V., García, M. A., Zaritzky, N. E. (2008). Film forming capacity of chemically modified corn starches. *Carbohydrate Polymers, 73(4),* 573-581.
16. Ninago, M. D., López, O. V., Lencina, M. M. S., García; M. A., Andreucetti, N. A. (2015). Enhancement of thermoplastic starch final properties by blending with poly(ε-caprolactone). *Carbohydrate Polymers, 134,* 205-212.
17. Piermaría, J., Bosch, A., Pinotti, A., Yantorno, O., García, M. A. et al. (2011). Kefiran films plasticized with sugars and polyols: water vapor barrier and mechanical properties in relation to their microstructure analyzed by ATR/FT-IR spectroscopy. *Food Hydrocolloids, 25,* 1261-1269.
18. Moreno-Osorio, L., Garcia, M., Villalobos-Carvajal, R. (2010). Effect of polygodial on mechanical, optical and barrier properties of chitosan films. *Journal of Food Processing and Preservation, 34(2),* 219-234.
19. Friedrich, F., Heissler, S., Faubel, W., Nüesch, R., Weidler, P. G. (2007). Cu(II)-intercalated muscovite: An infrared spectroscopic study. *Vibrational Spectroscopy, 43(2),* 427-434.
20. Cabrera, O. A. (2013). *Caracterización de la durabilidad de hormigones con arenas de trituración. (Ph.D. Thesis)*. Universidad Nacional Del Sur, Argentina.
21. Hunger, M., Brouwers, H. J. H. (2008). Natural stone waste powders applied to SCC mix design. *Buildings, 14(2),* 131-140.
22. Karmegam, A., Kalidass, A., Ulaganathan, D. (2014). Uporaba granitne prašine u samozbijajućem betonu. *Gradjevinar, 66(11),* 997-1006.
23. Singh, S., Naga,r R., Agrawal, V. (2016). A review on properties of sustainable concrete using granite dust as replacement for river sand. *Journal of Cleaner Production, 126,* 74-87.
24. Dang, K. M., Yoksan, R. (2016). Morphological characteristics and barrier properties of thermoplastic starch/chitosan blown film. *Carbohydrate Polymers, 150,* 40-47.
25. de Melo, C., Garcia, P. S., Grossmann, M. V. E., Yamashita, F., Dall'Antônia, L. H. et al. (2011). Properties of extruded xanthan-starch-clay nanocomposite films. *Brazilian Archives of Biology and Technology, 54(6),* 1223-1333.
26. Ninago, M. D., Lopez, O. V., Passaretti, M. G., Horst, M. F., Lassalle, V. L. et al. (2017). Mild microwave-assisted synthesis of aluminum-pillared bentonites thermal behavior and potential applications. *Journal of Thermal Analysis and Calorimetry, 129,* 1517-1531.
27. Sun, Q., Xi, T., Li, Y., Xiong, L. (2014). Characterization of corn starch films reinforced with $CaCO_3$ nanoparticles. *Plos One, 9(9),* 1-6.
28. Müller, C. M. O., Laurindo, J. B., Yamashita, F. (2012). Composites of thermoplastic starch and nanoclays produced by extrusion and thermopressing. *Carbohydrate Polymers, 89(2),* 504-510.
29. Edhirej, A., Sapuan, S. M., Jawaid, M., Zahari, N. I. (2017). Preparation and characterization of cassava bagasse reinforced thermoplastic cassava starch. *Fibers and Polymers, 18(1),* 162-171.
30. Chiou, B. S., Yee, E., Glenn, G. M., Orts, W. J. (2005). Rheology of starch-clay nanocomposites. *Carbohydrate Polymers, 59(4),* 467-475.

31. Park, H. M., Lee, S. R., Chowdhury, S. R., Kang, T. K., Kim, H. K. et al. (2002). Tensile properties, morphology, and biodegradability of blends of starch with various thermoplastics. *Journal of Applied Polymer Science, 86,* 2907-2915.
32. Savadekar, N. R., Mhaske, S. T. (2012). Synthesis of nano cellulose fibers and effect on thermoplastics starch based films. *Carbohydrate Polymers, 89(1),* 146-151.
33. Aila-Suárez, S., Palma-Rodríguez, H. M., Rodríguez-Hernández, A. I., Hernández-Uribe, J. P., Bello-Pérez, L. A. et al. (2013). Characterization of films made with chayote tuber and potato starches blending with cellulose nanoparticles. *Carbohydrate Polymers, 98(1),* 102-107.
34. Bodîrlău, R., Teacă, C. A., Spiridon, I., Tudorachi, N. (2012). Effects of chemical modification on the structure and mechanical properties of starch-based biofilms. *Monatshefte Für Chemie-Chemical Monthly, 143(2),* 335-343.
35. Castillo, L., López, O., López, C., Zaritzky, N., García, M. A. et al. (2013). Thermoplastic starch films reinforced with talc nanoparticles. *Carbohydrate Polymers, 95(2),* 664-674.
36. Mbey, J. A., Hoppe, S., Thomas, F. (2012). Cassava starch-kaolinite composite film. Effect of clay content and clay modification on film properties. *Carbohydrate Polymers, 88,* 213-222.
37. Khanoonkon, N., Yoksan, R., Ogale, A. A. (2016). Effect of stearic acid-grafted starch compatibilizer on properties of linear low density polyethylene/thermoplastic starch blown film. *Carbohydrate Polymers, 137,* 165-173.
38. Wang, L. F., Rhim, J. W. (2016). Grapefruit seed extract incorporated antimicrobial LDPE and PLA films: effect of type of polymer matrix. *LWT-Food Science and Technology, 74,* 338-345.
39. Jafarzadeh, S., Alias, A. K., Ariffin, F., Mahmud, S., Najafi, A. (2016). Preparation and characterization of bionanocomposite films reinforced with nano kaolin. *Journal of Food Science and Technology, 53(2),* 1111-1119.
40. Echeverría, I., Eisenberg, P., Mauri, A. N. (2014). Nanocomposites films based on soy proteins and montmorillonite processed by casting. *Journal of Membrane Science, 449,* 15-26.
41. Bertuzzi, M. A., Gottifredi, J. C., Armada, M. (2012). Mechanical properties of a high amylose content corn starch based film, gelatinized at low temperature. *Brazilian Journal of Food Technology, 15(3),* 219-227.